Radiation-enhanced diffusion of Sb and B in silicon during implantation below 400 °C

V. C. Venezia*
Philips Research Leuven, Kapeldreef 75, B-3001 Leuven, Belgium

L. Pelaz
Electronics Department, University of Valladolid, 47011 Valladolid, Spain

H.-J. L. Gossmann and Aditya Agarwal
Axcelis Technologies, Inc., 108 Cherry Hill Drive, Beverly, Massachusetts 01915, USA

T. E. Haynes
Condensed Matter Sciences Division, Oak Ridge National Laboratory, MS-6048, Oak Ridge, Tennessee 37831, USA
(Received 3 October 2003; published 24 March 2004)

We have investigated dopant-defect interactions during ion implantation of silicon into silicon by monitoring the radiation-enhanced diffusion (RED) of Sb and B dopant diffusion markers. The RED of these dopant markers has been investigated as a function of implant temperature (25–400 °C), implant dose (10^{14}–10^{16} cm^{-2}), and implant energy (2 MeV or 40 keV Si ions). Experimental results are interpreted with the aid of atomistic simulations that include detailed defect-defect and dopant-defect interactions. We demonstrate that RED of B and Sb occurs at lower temperatures than previously reported (below 100 °C and 200 °C, respectively) and the magnitude of this effect increases with implant temperature and dose. We also demonstrate that RED of these dopants is only measurable within the damage cascades of the implanted ions, i.e., there is no observable long-range diffusion of defects during implantation. Significant differences in dose, temperature, and depth dependence between B and Sb RED occur. Comparison of experimental and simulation results indicates that these differences are due to the diffusion mechanisms of the dopants. Simulations also demonstrate that the formation and dissolution of defect clusters during implantation plays a significant role in the observed temperature and dose dependencies.

DOI: 10.1103/PhysRevB.69.125215 PACS number(s): 61.72.Cc, 61.72.Ji, 61.80.Jh, 66.30.Jt

I. INTRODUCTION

Dopant-defect interactions in ion-implanted silicon have attracted considerable interest for both fundamental and technological reasons. Ion implantation is widely used for doping silicon in the fabrication of integrated circuits because of the precise control of dopant profiles it offers.[1,2] In addition to introducing dopant atoms into silicon, implantation also introduces lattice damage in the form of native point defects, such as Si self-interstitials and vacancies, as well as more complex defects. Hundreds to thousands of spatially correlated interstitial and vacancy pairs are generated within the collision cascade created by each implanted ion. The majority of these defects anneal during postimplant thermal processing via interstitial-vacancy recombination.

It is well known that dopant diffusion in silicon is mediated by native point defects.[3] Substitutional dopant atoms A_s migrate in silicon by pairing with either a Si self-interstitial I or a vacancy V, respectively, as follows:

$$A_s + I = AI \tag{1}$$

or

$$A_s + V = AV, \tag{2}$$

where AI is a dopant interstitial pair and AV is a dopant vacancy pair. It has been demonstrated that substitutional B diffuses almost entirely (98%) by an interstitial (cy) mechanism [Eq. (1)], while substitutional Sb diffuses almost entirely (99%) by a vacancy mechanism [Eq. (2)].[3,4] Thus an interstitial or vacancy supersaturation leads to a proportional enhancement in the diffusion of B or Sb, respectively.

Many recent investigations have shown that dopant-defect interactions during postimplant thermal processing are dominated by the net-excess defects induced by implantation, i.e., the defects that remain after all of the spatially correlated interstitials and vacancies have recombined. For instance, the transient enhanced diffusion (TED) of B is attributed to an excess of interstitial defects that remain after the primary interstitials and vacancies created by the implant have recombined.[3–8] For typical dopant implants and energies, the number of excess interstitials is approximately equal to the number of implanted ions.[7] Such a description of the net-excess point defects, also known as the plus one (“+1”) approximation,[8] has been used to model B TED with considerable success. Enhanced diffusion of Sb, a vacancy diffusing dopant, has been observed in the near surface region of silicon implanted with high-energy ions (MeV). In this case, an excess of vacancies over interstitials remains near the surface after recombination, while an excess of interstitials is present closer to the ions' projected range.

Although the net-excess defect concentrations are only a small fraction of the total defects created by a particular implant, they are responsible for large enhancements in dopant diffusion. As a result, the majority of dopant-defect studies have focused on interactions that occur during postimplant

anneals of implantation damage. In this work, dopant diffusion during implantation has been investigated. The mechanisms that are responsible for atomic diffusion in a solid during implantation can be generally described as ion-beam mixing.[9] The effect of temperature is crucial in identifying the mechanism of the observed atomic mixing.[10–13] For instance, at low temperatures, where defects and dopant impurities are not mobile (usually below 25 °C), the redistribution of atoms during ion irradiation (implantation) is dominated by collisional mixing.[9] That is, the atoms migrate by repeated collisional displacements within cascades of collisions induced by the implanted ion. Collisional mixing is independent of substrate temperature and only dependent on the material properties of the substrate, such as atomic mass, atomic number, and the effective displacement energy of the atoms.[10,11] At high substrate temperatures (>1000 °C) dopant diffusion during implantation is dominated by equilibrium diffusion, i.e., thermal defects, and is therefore temperature dependent but independent of implant conditions. At intermediate implant temperatures, atomic mixing is dominated by radiation-enhanced diffusion (RED). In this case, the observed dopant diffusion is due to dopant-defect pairs [Eqs. (1) and (2)], which are mobile during implantation.[9] As the defect concentrations created by the implanted ions are much larger than the equilibrium concentration, dopant diffusion during implantation is greatly enhanced. In this temperature regime, the defects created during implantation are mobile and anneal out by various mechanisms, such as migration to surfaces or internal sinks and direct recombination of interstitials and vacancies.[13] Thus the supersaturation of defects during implantation is set by the competition between defect generation, which is related to the dose rate, and defect annihilation, which depends on the mobility of the defects and therefore on substrate temperature.

Many ion-beam-mixing studies in crystalline silicon have been carried out with the use of broad implanted or prediffused dopant profiles of either interstitial or vacancy diffusing dopants at temperatures greater than 500 °C. Radiation-enhanced dopant diffusion in silicon during proton implantation has been previously reported for B, P, and As doped layers, where implant temperatures were greater than 500 °C.[14–16] In those studies the enhanced diffusion was observed to be independent of implant temperature, indicating that a steady-state defect concentration was reached for proton bombardment at these temperatures. The enhanced diffusion of Sb and B during self-implantation at temperatures greater than 500 °C has also been reported.[17,18]In these cases the enhancement in the Sb profile was also observed to be independent of temperature, while temperature dependence was observed during B implantation.

In this work, the RED of dopant markers was investigated between 25 °C and 400 °C. Dopant thermal diffusion and transient enhanced diffusion are minor effects at these temperatures, while defect diffusion and evolution are significant. Therefore, the observed RED of Sb and B markers in this work monitored the interaction of defect fluxes during ion implantation. Sb and B are used because of their complementary sensitivity during diffusion to vacancies and interstitials, respectively. The steep profile of the dopant markers

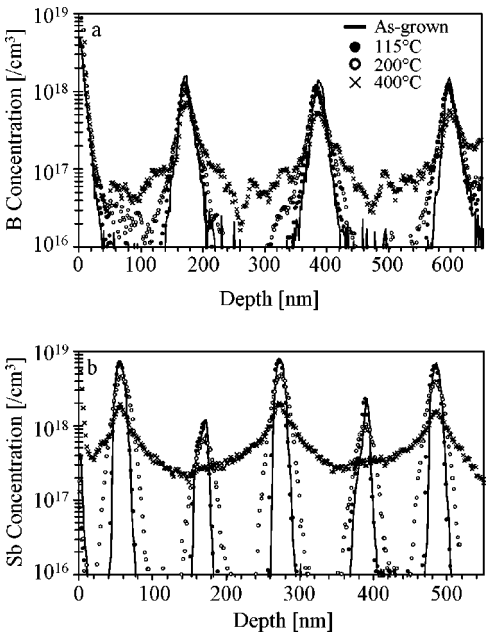

FIG. 1. SIMS depth profile of (a) B and (b) Sb marker samples implanted with 2 MeV Si ions to a dose of 10^{16} cm^{-2} at 115, 200, or 400 °C.

make it possible to detect small amounts of diffusion that occurred during implantation. The implants investigated are known to produce either a net excess of vacancies (2 MeV implants) (Refs. 19–21) or interstitials (40 keV implants) (Refs. 5 and 7) in the region of the dopant markers. The temperature and dose dependence of dopant diffusion during implantation have been investigated. The interpretation of the data is discussed on the basis of atomistic simulations that include detailed defect-defect and dopant-defect interactions.

II. EXPERIMENTAL AND SIMULATION CONDITIONS

Doping superlattices (DSL) containing a series of Sb- or B-doped layers grown by low-temperature molecular-beam epitaxy[22] on float-zone Si(100) substrates were used as diffusion markers. They either contained three markers of 2×10^{18} B cm^{-3} [Fig. 1(a)], five Sb markers grown to alternate between 10^{19} Sb cm^{-3} and 10^{18} Sb cm^{-3} [Fig. 1(b)], or a series of six 10-nm-thick B and Sb layers spaced 100 nm apart with concentrations of 2×10^{18} B cm^{-3} and 10^{19} Sb cm^{-3}, respectively (e.g., Fig. 4). All DSL's exhibited equilibrium diffusion after postgrowth annealing at temperatures ranging from 790 °C to 850 °C, indicating that the number of grown-in defects was negligible. A 1.7 MV tandem accelerator was used to implant samples with either 2 MeV or 40 keV $^{28}Si^{+}$ ions (projected range 1900 nm and 54 nm, respectively[21]) to a dose of 10^{14}, 10^{15}, or 10^{16} cm^{-2} with a fixed current of 0.22 μA cm^{-2}. Implants were performed at five different temperatures of 25, 115, 200, 300, and 400 °C. Samples were heated to these temperatures prior to implantation by an electric heater inside the sample holder and the temperature was maintained throughout the implant. Temperature was monitored by a thermocouple on the surface of a dummy sample placed alongside the sample of in-

terest and within the implanted area during each implant. Beam heating was therefore monitored and determined to be negligible. Dopant profiles were measured by secondary-ion mass spectrometry (SIMS) using a Cs^+ sputter beam for Sb DSL's and an O^- beam for B DSL's.

The determination of reliable diffusivities for the temperature and dose dependence of the Sb and B RED is dubious due to a number of complicating factors in the experimental data and complexities of interaction within the collision cascades. For instance, the diffusion is observed to be non-Fickian in nature, demonstrated by the low-concentration exponential tails. Similar diffusion behavior has been previously observed in low-temperature B diffusion experiments and is indicative of a minority population of mobile dopant-defect pairs that have large migration lengths.[23,24] However, application of this model is not straightforward due to the presence of intrinsic defect traps and those induced by the large concentrations of implantation-induced defects. Due to these effects the migration length is dependent on defect supersaturations and therefore on implant conditions. Immobile peaks observed in both the B and Sb diffusion profiles are indicative of dopant clustering, which also complicates the process of extracting meaningful diffusivities. In addition, defect recombination, defect clustering, defect trapping, and dopant-defect interactions, which all take place during implantation at elevated temperatures also complicate the accurate fitting of the RED profiles.

In light of the complications mentioned above, we have used an atomistic simulator (DADOS) (Ref. 25) to assist in the interpretation of the data and gain an understanding of the complex behavior of the observed Sb and B RED. In the simulations, the coordinates of interstitials and vacancies were transferred to a kinetic Monte Carlo routine from a collision cascade simulation (MARLOWE) based on the binary collision approximation.[26] Interstitials and vacancies were given random jumps at a rate derived from their diffusivities at the implant temperature. Interactions between particles leading to dopant diffusion, defect recombination, clustering and reemission from clusters, trapping, and detrapping with native traps (e.g., carbon and oxygen) were included in the simulations. Atoms were considered to interact when within a second-neighbor distance of each other. In addition, defects were created at the surface at a rate given by equilibrium injection, while all defects that arrived at the surface annihilated via surface recombination. These two processes fixed the surface-defect concentration at the thermal equilibrium values. The rates of all processes were determined by specific binding energies derived from molecular dynamics, first-principle calculations, and experiments. The Si self-diffusion coefficients[27] and the binding energy of interstitial clusters[28] were taken from experiments, whereas the binding energy for vacancy clusters were obtained from theoretical calculations.[29]

In the simulation, the concentration of dopant-defect pairs was determined by the availability of free defects [Eqs. (1) and (2)]. Since B diffuses by pairing with interstitials (and Sb with vacancies) the enhanced B (Sb) diffusivity is proportional to the number of interstitial (vacancy) ''hops'' per lattice site, which is a measure of the number of opportunities for a dopant atom to pair with an interstitial (vacancy). The number of interstitial B (BI) hops is proportional to the amount of B diffusion and the number of interstitial and vacancy hops is proportional to the time-averaged concentration of these free, mobile point defects, and therefore, to the diffusion of interstitial or vacancy diffusing dopants.[30] Therefore, the diffusion is analyzed in terms of point defects or dopants hops.

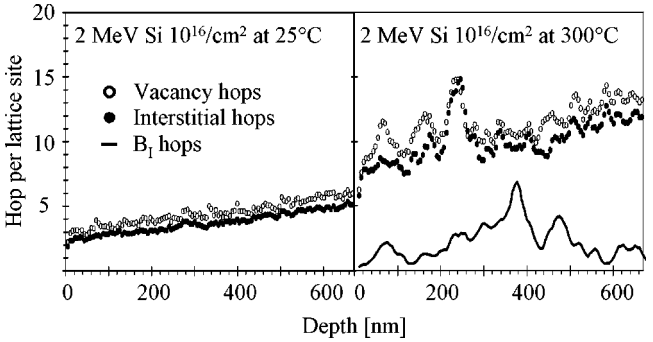

FIG. 2. Plot of the number of hops per lattice site of Si interstitials, vacancies, and interstitial B vs depth for a 2 MeV, 10^{16} cm^{-2} Si implant into a B DSL at (a) 25 °C and (b) 300 °C, as simulated by DADOS.

III. TEMPERATURE DEPENDENCE OF RADIATION-ENHANCED DIFFUSION

In order to determine the mechanism responsible for diffusion of Sb and B atoms during implantation at temperatures from 25 to 400 °C, the temperature dependence of diffusion during implantation was first investigated. No measurable amount of diffusion occurred for either Sb or B when the implant temperature was held at 25 °C (data not shown). Figure 1 contains Sb and B concentration profiles for samples implanted with 2 MeV Si ions to a dose of 10^{16} cm^{-2} at 115, 200, and 400 °C. There are several observations of interest in Fig. 1. First, both the Sb and B dopant markers exhibit a large enhanced diffusion relative to their equilibrium diffusion lengths at the implant temperatures (<0.1 nm for both B and Sb).[3] Second, the amount of enhanced diffusion for both dopants is temperature dependent. However, the temperature dependence is not the same: B diffusion is observed in the samples implanted at 115 °C, while Sb diffusion is not observed for that annealing temperature, yet it is observed when the implant temperature is 200 °C. Based on the temperature dependence and large diffusion enhancements observed in Fig. 1, both collisional mixing and thermal diffusion are ruled out as the dominant mechanisms of the dopant redistribution. It is concluded from the data that RED dominates the atomic mixing occurring in these experiments, that is, defect-mediated diffusion occurs during implantation.

Simulation results for a 2 MeV, 10^{16} Si cm^{-2} implant into a B DSL at 25 °C and at 300 °C are shown in Fig. 2. In the figure the number of diffusion hops per lattice site of isolated interstitials, vacancies, and interstitial B (B_I) atoms that occur during the implant are plotted versus depth. For the same

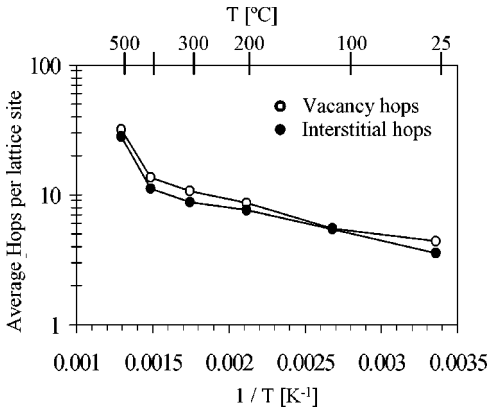

FIG. 3. Plot of the average number of interstitial or vacancy hop concentration per lattice site integrated over the depth that covers the dopant markers vs inverse temperature during a 2 MeV, 10^{16} cm^{-2} Si implant into silicon as simulated by DADOS.

energy and dose, implantation at 300 °C results in only a slight increase in the number of mobile interstitials and vacancies compared to implantation at 25 °C. In the experimental data, B diffusion occurs for the elevated temperature implant. The results in Fig. 2 are understood in terms of the detailed mechanisms of B diffusion. For instance, a substitutional B atom (B_s) must first pair with a Si interstitial to form a B-interstitial (BI) pair. *Ab initio* calculations by Zhu *et al.*,[31] indicate that the BI pair is a low mobility configuration. The BI pair must surmount an energy barrier of 1 eV to reach a higher mobility state, the B_I configuration. Considering that the 10^{16} cm^{-2} implant took $\approx 10^3$ s, a BI complex with vibrational frequency of 10^{13} s^{-1} makes 10^{16} attempts during the implant to surmount the 1 eV energy barrier.[30] The probability of the BI pair surmounting an energy barrier E at a given temperature T is proportional to $\exp(-E/k_BT)$, where k_B is the Boltzmann constant. The number of successful attempts becomes significant (larger than 1), when the substrate temperature is greater than 40 °C.[32] Therefore, although a large concentration of free interstitials is present for both conditions in Fig. 3, only the dopant-defect pairs that form at the higher temperature can become mobile. This reasoning is consistent with the experimental data in Fig. 2, in which B RED only occurs for the substrate temperatures greater than 25 °C.

The simulation used in this work did not include detailed mechanisms for Sb diffusion. However, we can apply the above reasoning to the case of Sb diffusion, whereby a substitutional Sb atom must pair with a free vacancy defect to diffuse. Experimental and theoretical results indicate that the migration energy of the Sb-V pair is 1.3–1.4 eV.[33,34] With a migration energy in this range, the substrate temperature would have to be ≈150 °C or greater during the 2 MeV Si implant for the Sb-V pairs to diffuse, consistent with our experimental results.

Above the temperature at which the dopant-defect pairs become mobile, the amount of RED is affected by the concentration of free defects created during the elevated temperature implants. Figure 3 is a plot of the average concentration of interstitial and vacancy hops for simulations of 2 MeV, 10^{16} cm^{-2} Si implanted into a silicon substrate at temperatures ranging from 25 to 500 °C. The increase in defect hops with increased temperature indicates that more free defects are available to enhance dopant diffusion during implantation at higher substrate temperature. In the simulation, we assume that the number of interstitial-vacancy pairs produced in each cascade is independent of the implant temperature. The difference in the number of free interstitial or vacancy hops is explained by the presence of defect traps and by the clustering and Ostwald ripening of defect clusters. At low temperatures, interstitials and vacancies generated during implantation can agglomerate into small immobile clusters and/or be trapped by C (Ref. 35) or O (Ref. 36) respectively, which are present in our samples to concentrations of 10^{17} C cm^{-3} and 10^{18} O cm^{-3}. As the implant temperature is increased, defects are released from these traps and from small clusters as they anneal; for example, vacancy-oxygen and vacancy-vacancy pairs anneal above 300 °C. The temperature dependence in Sb and B RED, observed experimentally in Fig. 1, is most likely due to the differences in emission rates of defects from traps and clusters at the different implant temperatures.

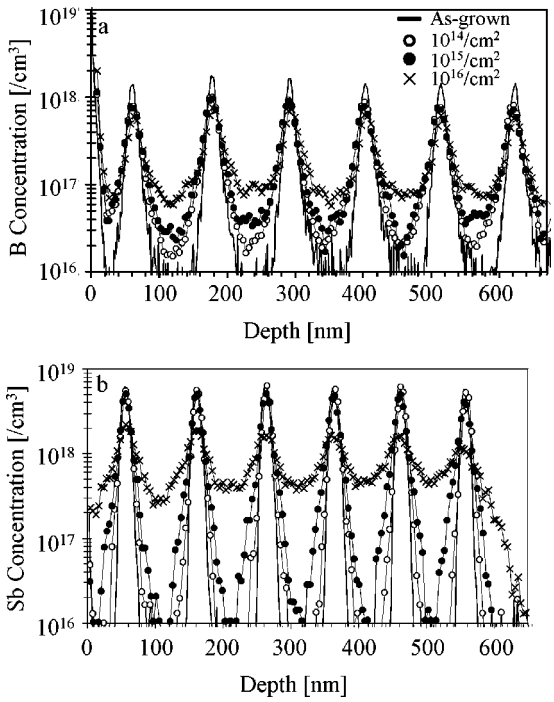

FIG. 4. SIMS depth profile of (a) B and (b) Sb DSL implanted with 2 MeV Si ions to a dose of 10^{14}, 10^{15}, or 10^{16} cm^{-2} at 300 °C.

IV. DOSE DEPENDENCE OF RADIATION-ENHANCED DIFFUSION

The amount of RED is also observed to be dependent on implant dose. Figure 4 contains the concentration profiles of B and Sb DSL's implanted with 2 MeV Si ions at 300 °C to a dose of 10^{14}, 10^{15}, or 10^{16} cm^{-2}. The amount of diffusion is observed to increase for both B and Sb as the dose increases, consistent with an increase in the concentration of implantation-induced defects. It is interesting to note that

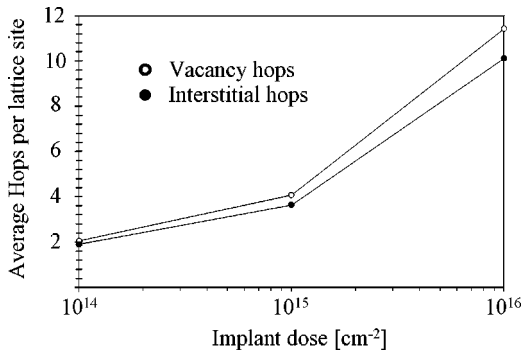

FIG. 5. Plot of the average number of interstitial or vacancy hops per lattice site over the depth that covers the dopant markers vs implant dose during a 2 MeV Si implant into silicon at 300 °C, as simulated by DADOS.

even for the lowest dose of 10^{14} cm^{-2} there is a measurable amount of RED for both Sb and B markers. However, the amount by which the diffusion is increasing with dose is different for Sb and B. The RED of B is more significant at lower doses than Sb. The RED of Sb increase only slightly from 10^{14} to 10^{15} cm^{-2} and much more drastically between the 10^{15} and 10^{16} cm^{-2} implants.

Figure 5 is a plot of the average interstitial or vacancy hops in the region of the dopant markers as a function of dose for a 2 MeV Si implant at a substrate temperature of 300 °C. Since the temperature of the substrate is above that at which RED occurs for Sb and B, these simulation results predict that the amount of RED would increase with implant dose, consistent with experimental observations. Because of the competition between recombination, defect clustering, and trapping, it is not surprising that the RED does not increase linearly with dose, or that the amount of increase would be the same for Sb and B, since their diffusion involves different types of defects.

The immobile fraction of the Sb and B peaks in Figs. 1 and 4 are indications that clustering of these dopants has occurred during the 2 MeV Si implants. Atomistic simulations have previously suggested that the clustering of ion-implanted B proceeds from a precursor complex of B and silicon interstitial atoms (BI_2) which forms during implantation in the presence of the high concentrations of silicon interstitials and vacancies that exist prior to recombination.[37] The presence of a fraction of immobilized B atoms in the RED data even at the highest temperatures and the highest doses used is thus consistent with the formation of B complexes, as predicted by that model. Defect-assisted Sb clustering has also been previously observed in implanted Sb profiles. Investigations demonstrate that the fraction of deactivated Sb, in an Sb implanted profile, after annealing at low temperature (<850 °C) is predominantly found in Sb-V complexes and at higher temperatures (>850 °C) in precipitates of higher-order Sb-V complexes.[38] It is reasonable that the large concentrations of vacancies created during implantation in this work can readily pair with substitutional Sb atoms, and the mobile Sb-V pairs and vacancies can make these Sb-V pairs grow to higher-order clusters during implantation, similar to the case of B clustering.

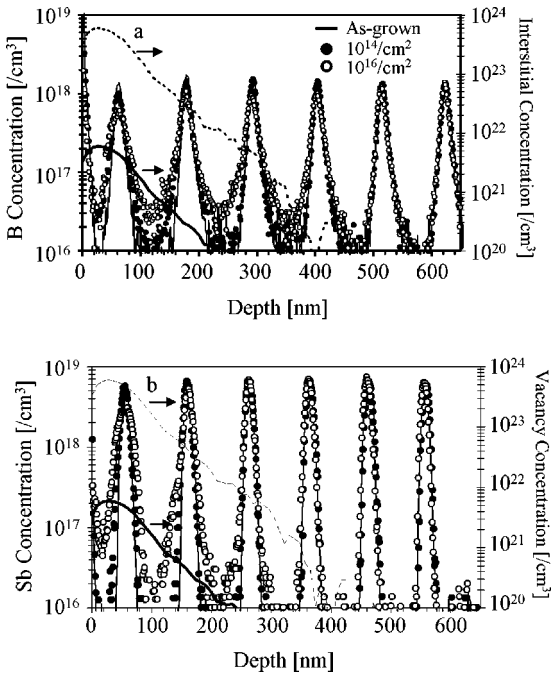

FIG. 6. SIMS depth profiles of (a) B and (b) Sb DSL implanted with 40 keV Si ions to a dose of 10^{14} or 10^{16} cm^{-2} at 300 °C. Included in each figure are the interstitials (in 3a) or vacancy (in 3b) profiles generated by a 40 keV Si implant of dose 10^{14} (darker solid line) and 10^{16} cm^{-2} (dashed line).

V. EFFECT OF LOW-ENERGY IMPLANT ON RADIATION-ENHANCED DIFFUSION

In Secs. III and IV, Sb and B RED were observed when high-energy ions were implanted through the dopant markers. Figure 6 contains B and Sb profiles of samples implanted with medium energy, 40 keV Si ions at 300 °C to doses of 10^{14} and 10^{16} cm^{-2}. Because of the elevated implant temperature, amorphizaton is prevented even in the highest dose case. Also included in the figure is the interstitial or vacancy profile of these implants as predicted by MARLOWE.[26] For these implant conditions, the ions come to rest inside the region of the dopant markers. RED is observed for both Sb and B after the 40 keV Si implant, similar to that observed in the MeV Si implanted samples. However, in this case only the shallow Sb and B markers that are within the damage profile exhibit RED, demonstrating that the depth to which this effect is measurable scales with the depth of the damage profile created by the implanted ions.

Figure 7 is a plot of the vacancy-, interstitial-, and interstitial B- hop concentration for a simulation of a 40 keV Si implant into a B DSL at 300 °C to a dose of 10^{14} cm^{-2}, Fig. 7(a), or 10^{16} cm^{-2}, Fig. 7(b). For B, the depth dependence of diffusion (the BI hops) tracks the interstitial-hop concentration profile. The defect-hop profile only extends as far as the damage profile of the 40 keV Si implant, as predicted by MARLOWE (shown as the dashed and dark solid lines in Fig. 6). Thus the defects that are created during implantation are only mobile and able to enhance dopant diffusion for a short time and distance after creation due to rapid recombination and/or trapping. Although a low-energy implant re-

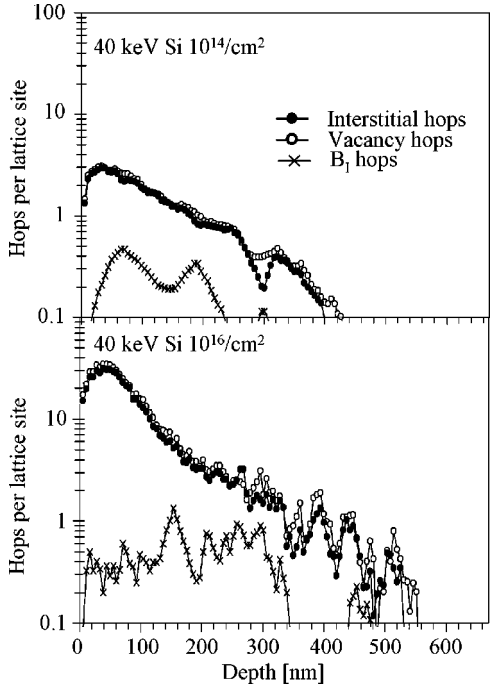

FIG. 7. Plot of the interstitial, vacancy and interstitial B hop concentrations vs depth during a 40 keV Si implant into a B DSL at 300 °C to a doses of (a) 10^{14} cm^{-2} and (b) 10^{16} cm^{-2}.

sults in an interstitial excess in the region of the dopant markers, Fig. 7 shows similar number of hops for interstitials and vacancies. This is because we are monitoring the hops during the implant produced by the total generated defects and not only the excess defects. However, the RED of B is observed to occur $\approx$100 nm deeper than it occurs for Sb during a 40 keV Si implant at 300 °C, Fig. 6. Since the activation energy for Sb diffusion is larger than it is for B,[3] a higher concentration of vacancies are needed to cause Sb RED than the concentration of interstitials that are needed to result in a similar B RED. The shallower RED of Sb markers, when compared to B markers, may therefore be a result of the concentration of vacancies in the tail of the 40 keV profile being too low to result in a measurable amount of Sb RED. Also, as discussed previously, the different trapping mechanisms for interstitials and vacancies may result in a lower concentration of mobile vacancies over interstitials. The depth to which B RED is observed in this work is consistent with the depth to which interstitial deactivation of B in CZ silicon is observed for a similar 40 keV Si implant.[39] In that work, the deactivation of B during room-temperature implantation was attributed to the interstitials pairing with the B atoms to form B-I pairs, which are stable at room temperature.

VI. RADIATION-ENHANCED DIFFUSION AND TRANSIENT ENHANCED DIFFUSION

For both Sb and B, RED was observed when DSL's were implanted with 40 keV Si ions or with 2 MeV Si ions. Many experiments have demonstrated that implantation of Si with such a 40 keV Si implant produces a net excess of interstitials in the region of the dopant markers, resulting in enhanced B diffusion during postimplant annealing. An enhanced Sb diffusion has been observed after postimplant annealing of a 2 MeV Si implant into similar Sb DSL's as used in this work. Implantation of silicon with MeV Si ions has also been shown to eliminate the interstitial excess that causes B TED. These experiments indicate that an excess of vacancy-type defects results in the near surface (the dopant marker region) region of silicon implanted by high-energy Si ions. Although the net-excess defects from the 40 keV and 2 MeV Si implant are complementary, interstitials versus vacancies, RED is observed for both Sb and B for both implants. This observation indicates that the dopant diffusion during implantation in these experiments proceeds from dopant-defect pairing prior to recombination and is therefore related to the initial or total defect profile created by the damage cascades of the implanted ions, rather than the net excess that is responsible for TED.

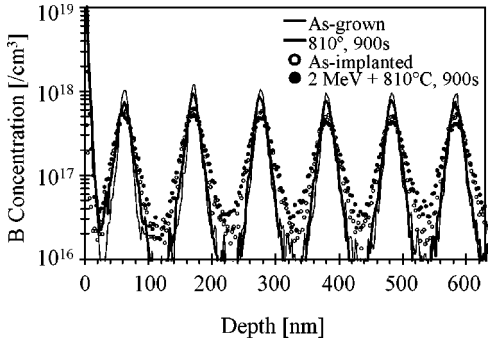

FIG. 8. SIMS depth profiles of a B DSL: as-grown, annealed at 800 °C for 900 s, implanted with 2 MeV Si ions to a dose of 10^{16} cm^{-2} at 60 °C (as-implanted), and 2 MeV Si implanted and annealed at 810 °C for 900 s.

Figure 8 demonstrates diffusion occurring prior to recombination of interstitial-vacancy pairs (RED) and after recombination (TED), i.e., the net excess. The figure shows concentration profiles of B DSL implanted with 2 MeV Si ions to a dose of 10^{16} cm^{-2} at 60 °C, where one sample was subsequently annealed at 810 °C for 900 s. Included in the figure is the as-grown or initial B profile and the profile from a sample which was not implanted but was annealed at 810 °C for 900 s, as a reference. Comparing the as-grown profile to the as-implanted profile, it is clear that some RED occurred during self-implantations. As a result, the profile from the MeV-implanted and annealed sample is a convolution of the RED and the diffusion after postimplant annealing. To account for RED, the profile of the implanted and annealed sample must be compared to that of the as-implanted profile, not the as-grown profile, to extract a correct diffusivity. Diffusivities were extracted by solving the diffusion equation derived from the kickout mechanism with the resulting concentration dependent diffusivity as variable. An optimization shell varies the diffusivity until the best fit between experimental diffused profile and simulated diffused profile is found.[40] When this is done, as shown in Fig. 9, it is clear that after implantation there is no further enhancement in B diffusion as a result of annealing. Therefore, there is no

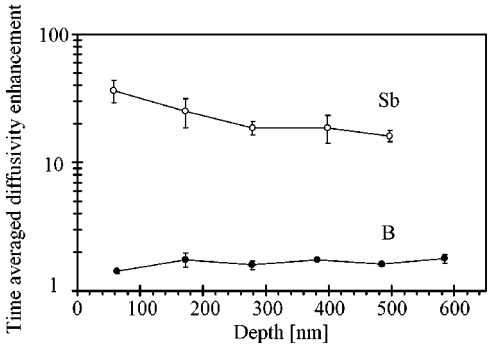

FIG. 9. Time-averaged diffusivity enhancements vs depth for a Sb and B DSL implanted with 2 MeV Si ions to a dose of 10^{16} cm^{-2} at 60 °C followed by an 810 °C, 900 s anneal, time-averaged diffusivity enhancements were extracted by a diffusion simulation routine that evolves an initial profile into a diffused profile. Enhancements are relative to thermal equilibrium values.

appreciable interstitial supersaturation in this region after recombination.[41]

When this same experiment was done with Sb DSL's, no measurable RED was observed, but a $\sim 20\times$ enhancement in Sb diffusion occurred during the 810 °C anneal, Fig. 9. It is thus concluded that after recombination is complete this region is dominated by a net excess of vacancy-type defects. Our observations are in contrast to the suggestion made in Ref. 20 that diffusion of both Sb and B were enhanced during an 810 °C anneal after the 2 MeV Si implant. Based on the experiments reported in this paper, it is likely that the diffusion of B observed in that experiment was largely dominated by RED. Unfortunately the as-implanted profiles were not measured in that experiment, and the diffusivity was extracted by comparing directly the as-grown B and Sb profiles to those after anneal.

VII. CONCLUSIONS

In this work the diffusion of dopants during implantation at elevated temperatures (>25 °C) was investigated. This diffusion was shown to be temperature dependent and enhanced over equilibrium (thermal) diffusion, and was determined to be RED dominated. The RED of both Sb and B was observed for implanted ions that pass through these dopant markers, 2 MeV Si ions, and for implants that come to rest inside the dopant markers, 40 keV Si implants. With the aid of Monte Carlo simulations that account for defects generated during implantation and dopant-defect pairing, the temperature, dose, and energy dependence of RED was explained. For a given dopant, the onset of RED is dependent on the specific energetics of the dopant-defect pair. For instance, the energy barrier to form a mobile B-interstitial complex is lower than that of a mobile Sb-V complex, resulting in RED of B occurring at a lower temperature than for the Sb case. Above the temperature at which mobile dopant-defect pairs form, the temperature dependence of RED is due to that of the free defect concentration, which is determined by the energetics of defect clustering and trapping and detrapping. RED occurs within the damage cascade of the implant, and is therefore depth dependent with the energy of the implant. Investigations of Sb and B, complementary diffusing dopants, demonstrate that RED is caused by the defects generated during implantation, prior to recombination or trapping. Since the total number of Frenkel pairs is much larger than the excess defect generated by the implant, RED is independent of the type of excess defect (interstitial or vacancy) present in the damaged region. Therefore, it appears both for interstitial and vacancy diffusing dopants. During implantations at low temperatures defects accumulate without much diffusion or interaction. During the postimplant anneals their recombination takes place quickly within few diffusion hops and only the excess of one defect over the other remains. These defects cluster and dissolve by diffusion to and annihilation at the surface. On their way to the surface, the excess defects may interact with dopant atoms causing enhanced diffusion. Therefore, only dopants that interact with the excess defect will diffuse during postimplant thermal processing. The total diffusion observed for coimplanted dopants in silicon at even moderately elevated temperatures (>25 °C), followed by postimplant annealing at higher temperature is therefore a convolution of diffusion occurring prior to defect recombination, RED, and after recombination has occurred, TED.

ACKNOWLEDGMENTS

The authors wish to acknowledge the contributions of D. C. Jacobson and D. J. Eaglesham. Research at Oak Ridge National Laboratory was sponsored by the U.S. Department of Energy, Office of Science, Laboratory Technology Research Division and the Division of Materials Sciences under Contract No. DE-AC05-00OR22725 with UT-Battelle, LLC.

*Electronic address: vincent.venezia@philips.com

[1] The National Technological Roadmap for Semiconductors, Semiconductor Industry Association.

[2] E. Chanson *et al.*, J. Appl. Phys. **81**, 6513 (1997).

[3] P.M. Fahey, P.B. Griffin, and J.D. Plummer, Rev. Mod. Phys. **61**, 289 (1989).

[4] H.-J. Gossmann, T.E. Haynes, P.A. Stolk, D.C. Jacobson, G.H. Gilmer, J.M. Poate, H.S. Luftman, T.K. Mogi, and M.O. Thompson, Appl. Phys. Lett. **71**, 3862 (1997).

[5] P.A. Stolk, H.-J. Gossmann, D.J. Eaglesham, D.C. Jacobson, C.S. Rafferty, G.H. Gilmer, M. Jaraiz, J.M. Poate, H.S. Luftman, and T.E. Haynes, J. Appl. Phys. **81**, 6031 (1997).

[6] M. Jaraiz, G.H. Gilmer, J.M. Poate, and T.D. de la Rubia, Appl. Phys. Lett. **68**, 409 (1996).

[7] D.J. Eaglesham, P.A. Stolk, H.-J. Gossmann, and J.M. Poate, Appl. Phys. Lett. **65**, 2305 (1994).

[8] M.D. Giles, J. Electrochem. Soc. **138**, 1160 (1991).

[9] S.M. Myers, Nucl. Instrum. Methods **168**, 256 (1980).

[10] S. Matteson, B.M. Paine, M.G. Grimaldi, G. Mezey, and M.A. Nicolet, Nucl. Instrum. Methods **182/183**, 43 (1981).

[11] S. Matteson, B.M. Paine, and M.A. Nicolet, Nucl. Instrum. Methods **182/183**, 53 (1981).

[12] L. Pelaz, V.C. Venezia, G.H. Gilmer, H.-J. Gossmann, M. Jaraiz, and J. Barbolla, Appl. Phys. Lett. **74**, 2017 (1999).
[13] G. Dienes and A.C. Damask, J. Appl. Phys. **29**, 1713 (1958).
[14] D. Nelson, J.F. Gibbons, and W.S. Johnson, Appl. Phys. Lett. **14**, 246 (1969).
[15] B.J. Masters and E.F. Gorey, J. Appl. Phys. **49**, 2017 (1978).
[16] P. Leveque, J. Christensen, A.Y. Kuznessov, B. Svensson, and A.N. Larsen, J. Appl. Phys. **91**, 4073 (2002).
[17] K. Gamo, K. Masuda, S. Namba, S. Ishihara, and I. Kimura, Appl. Phys. Lett. **17**, 391 (1970).
[18] R. Schork, P. Pichler, A. Kluge, and H. Ryssel, Nucl. Instrum. Methods Phys. Res. B **59/60**, 499 (1991).
[19] V.C. Venezia, D.J. Eaglesham, T.E. Haynes, A. Agarwal, D.C. Jacobson, H.-J. Gossmann, and F. Baumann, Appl. Phys. Lett. **73**, 2980 (1998).
[20] D.J. Eaglesham, T.E. Haynes, H.-J. Gossmann, D.C. Jacobson, P.A. Stolk, and J.M. Poate, Appl. Phys. Lett. **70**, 3281 (1997).
[21] J.F. Ziegler, J.P. Bierszack, and U. Littmark, *The Stopping and Ranges of Ions in Solids* (Pergamon, New York, 1985).
[22] H.-J. Gossmann, F.C. Unterwald, and H.S. Luftman, J. Appl. Phys. **73**, 8237 (1993).
[23] N.E.B. Cowern, G.F.A. van de Walle, D.J. Gravesteijn, and C.J. Vriezema, Phys. Rev. Lett. **67**, 212 (1991).
[24] N.E.B. Cowern, K.T.F. Janssen, G.F.A. van de Walle, and D.J. Gravesteijn, Phys. Rev. Lett. **65**, 2434 (1990).
[25] M. Jaraiz, L. Pelaz, J.E. Rubio, J. Barbolla, G.H. Gilmer, D.J. Eagesham, H.-J. Gossmann, and J.M. Poate, in *Silicon Front-End Technology—Materials Processing and Modelling*, edited by N.E.B. Cowern, D. Jacobson, P. Griffin, P. Packan, and R. Webb, Mater. Res. Soc. Symp. Proc. No. 532 (Materials Research Society, Pittsburgh, 1998), p. 43.
[26] M.T. Robinson and I.M. Torrens, Phys. Rev. B **9**, 5008 (1974).
[27] H. Bracht, E.E. Haller, and R. Clark-Phelps, Phys. Rev. Lett. **81**, 393 (1998).
[28] N.E.B. Cowern, G. Mannino, P.A. Stolk, F. Roozeboom, H.G.A. Huizing, J.G.M. van Berkum, F. Cristiano, A. Claverie, and M. Jaraiz, Phys. Rev. Lett. **82**, 4460 (1999).
[29] A. Bongiorno, L. Colombo, and T.D. de la Rubia, Europhys. Lett. **43**, 675 (1998).
[30] For example, D.R. Olander, *Fundamental Aspects of Nuclear Fuel Elements* (ERDS, Technical Information Center, Oak Ridge, TA, 1976), Chap. 7.
[31] J. Zhu, T.D. de la Rubia, L.H. Yang, C. Maihiot, and G.H. Gilmer, Phys. Rev. B **54**, 4741 (1996).
[32] $\exp[-E/k_BT] > 10^{-16}$ when $T \sim 40\,^{\circ}\mathrm{C}$ (313 K), E (the energy barrier) is 0.85–1 eV, and k_B is the Boltzmann constant.
[33] J.S. Nelson, P.A. Schultz, and A.F. Wright, Appl. Phys. Lett. **73**, 247 (1998).
[34] M. Hirata, M. Hirata, and H. Saito, J. Phys. Soc. Jpn. **27**, 405 (1969).
[35] L.W. Song, X.D. Zhan, B.W. Benson, and G.W. Watkins, Phys. Rev. B **42**, 5765 (1990).
[36] J.W. Corbett, G.D. Watkins, R.M. Chrenko, and R.S. McDonald, Phys. Rev. **121**, 1015 (1961).
[37] L. Pelaz, M. Jaraiz, G. Gilmer, H.-J. Gossmann, C.S. Rafferty, D. Eaglesham, and J. Poate, Appl. Phys. Lett. **70**, 2285 (1997).
[38] G. Weyer, A.N. Larsen, N.E. Holm, and H.L. Nielson, Phys. Rev. B **21**, 4939 (1980).
[39] K.K. Larsen, V. Privitera, S. Coffa, S.U.C.F. Priolo, and A. Carbera, Phys. Rev. B **76**, 1494 (1996).
[40] H.-J. Gossmann, A.M. Vredenberg, C.S. Rafferty, H.S. Luftman, F.C. Unterwald, D.C. Jacobson, T. Boone, and J.M. Poate, J. Appl. Phys. **74**, 3150 (1993).
[41] V.C. Venezia, T.E. Haynes, A. Agarwal, L. Pelaz, H.-J. Gossmann, D.C. Jacobson, and D.J. Eaglesham, Appl. Phys. Lett. **74**, 1299 (1999).